REPORT DOCUMENTATION PAGE

Form Approved OMB No. 0704-0188

1. REPORT DATE *(DD-MM-YYYY)* 09-03-2004	2. REPORT TYPE Final Report	3. DATES COVERED *(From – To)* 27 September 2002 - 27-Sep-03

4. TITLE AND SUBTITLE

A Variable Stiffness Concept For Efficient Aircraft Vertical Tail Design

5a. CONTRACT NUMBER
FA8655-02-1-3085

5b. GRANT NUMBER

5c. PROGRAM ELEMENT NUMBER

6. AUTHOR(S)

Professor Jonathan E Cooper

5d. PROJECT NUMBER

5d. TASK NUMBER

5e. WORK UNIT NUMBER

7. PERFORMING ORGANIZATION NAME(S) AND ADDRESS(ES)
University of Manchester
Oxford Road
Manchester M13 9PL
United Kingdom

8. PERFORMING ORGANIZATION REPORT NUMBER

N/A

9. SPONSORING/MONITORING AGENCY NAME(S) AND ADDRESS(ES)

EOARD
PSC 802 BOX 14
FPO 09499-0014

10. SPONSOR/MONITOR'S ACRONYM(S)

11. SPONSOR/MONITOR'S REPORT NUMBER(S)
SPC 02-4085

12. DISTRIBUTION/AVAILABILITY STATEMENT

Approved for public release; distribution is unlimited.

13. SUPPLEMENTARY NOTES

14. ABSTRACT

This report results from a contract tasking University of Manchester as follows: The contractor will investigate using a variable stiffness vertical tail attachment to control aeroelastic performance over a range of dynamic pressures. The contractor will (1) Develop an adaptive stiffness attachment for vertical tail aircraft; (2) Develop an analytical model of the attachment and predict aeroelastic performance; (3) Design, build and test a vertical tail model with and without a rudder to demonstrate the concept and validate the theoretical predictions; and (4) Conduct wind tunnel testing at sub and supersonic Mach Numbers; and (5) Consider the extension of the design for full-size aircraft and to quantify the benefits.

15. SUBJECT TERMS
EOARD, Aircraft Design, Aerodynamics, Aeroelasticity

16. SECURITY CLASSIFICATION OF:			17. LIMITATION OF ABSTRACT	18, NUMBER OF PAGES	19a. NAME OF RESPONSIBLE PERSON WAYNE A. DONALDSON
a. REPORT UNCLAS	**b. ABSTRACT** UNCLAS	**c. THIS PAGE** UNCLAS	UL	30	19b. TELEPHONE NUMBER *(Include area code)* +44 (0)20 7514 4299

Standard Form 298 (Rev. 8/98)
Prescribed by ANSI Std. Z39-18

FINAL REPORT

A Variable Stiffness Concept For Efficient Aircraft Vertical Tail Design

EOARD CONTRACT FA8655-02-1-3085

Professor J E Cooper, Professor O Sensburg, M. Amprikidis

School of Engineering
University of Manchester
Oxford Road, Manchester, M13 9PL, UK.

29th September 2003

Summary

This report describes the work undertaken for the EOARD contract FA8655-02-1-3085 on "A Variable Stiffness Concept For Efficient Aircraft Vertical Tail Design". It involved the design and manufacture of variable torsional stiffness attachments for a vertical tail wind tunnel model. A vertical tail wind tunnel model was bench and also wind tunnel tested to examine the capabilities of the adaptive stiffness attachments. There were some setbacks on the actual designs which led to excessive freeplay and permanent deformations, however, successful testing was achieved in one of the test set-ups and it was shown that it is possible to control the torsional stiffness with the manufactured device. Comparisons with results from the analytical studies correlated well. An improved design of the adaptive attachment has been made which will fulfill the requirements for such a device.

Introduction

The conventional design practice for aerospace structures such as aircraft fins is to build very stiff structures, and consequently minimizing the elastic structural deflections. This approach reduces the likelihood of any undesirable aeroelastic phenomena. An opportunity for a paradigm shift has arisen in the design philosophy whereby these elastic deflections can now be used to enhance the aerodynamic performance[1,2].

Such a philosophy will lead to large weight savings, or improvements in other aeroelastic constraints (flutter, divergence, vibration response, etc.) In order to achieve these goals, it is necessary to approach the problem in a multi-disciplinary manner employing the so-called Multi-Disciplinary Design Optimization (MDO) methodology [3]. It is not possible to achieve an optimal design without using MDO due to the conflicting demands of different technical disciplines. This approach is being used in the Active Aeroelastic Wing (AAW) and Active Aeroelastic Aircraft Structures (3AS) research programs.

Previous work (funded by the EOARD) undertaken by the investigator, examined the design of a generic all-moveable fin using the Lagrange aeroelastic optimization package [4,5]. This study showed that it was possible to improve the aeroelastic effectiveness of the vertical tail through variation of the fin and attachment stiffness.

A follow-on AFOSR funded project demonstrated the concept experimentally. A wind tunnel model was created using the carbon fiber vertical tail, shown in fig. 1, was available for this work and was modified to represent an all-movable vertical tail. Different attachment stiffnesses and positions were considered, with the results validating the theoretical predictions. Attaching it to the ground with soft springs made it feasible to simulate high efficiencies at the rear attachment position for the low dynamic pressures of a subsonic wind tunnel (see fig. 3). Through the use of similarity laws it is possible to extend the results to that of a full-scale fin.

These studies showed that it is desirable to use attachments with variable stiffness, in order to be able to achieve good static aeroelastic behaviour even at low speeds whilst satisfying dynamic aeroelastic constraints – flutter and divergence at high speeds (see fig. 2).

Design and Manufacture of An Adaptive Torsional Stiffness Attachment

The aim of this research proposal is to develop a concept for a vertical aircraft tail with variable torsional stiffness. In order to exploit the aeroelastic deformation at low speeds, it is necessary to create an attachment stiffness that is able to vary by about a factor of 40 lower from the original stiffness (deduced from figure 2). Since we have a pivoted structure on the vertical tail with a distinct loadpath, such a goal is much easier to perform than that on an overdetermined attachment such as with wings or conventional vertical tails.

The concept evaluated allowed a variation in the length of the beam in torsion that attaches the all-moving vertical tail. This effectively varies the torsional stiffness of the attachment, as seen in figure 4. Figure 5 shows an idealized schematic as to how the concept might be incorporated onto a full size aircraft. Two types of adaptive stiffness devices were manufactured, one based upon a solid square shape and the other on four rods, and are shown in figures 6 and 7.

Initial Analysis for Design of Adaptive Stiffness Attachment for All-Moving Vertical Tail

The Adaptive Stiffness Attachment was demonstrated upon the wind tunnel model that had been used in the previous studies investigating the effect of position and torsional stiffness of the single attachment. Consequently, the attachment had to be designed such that a reasonable amount of deflection was obtainable; not too little as to be difficult to measure accurately, but also not too large so that excessive twist might lead to problems with the attachment of the airflow around the fin (divergence may also occur).

The simplified analysis used here is intended to provide some initial calculations regarding the design of the torsional attachment. It was felt that at this initial stage there was no need to perform a more accurate finite element based analysis at this stage of the research programme in terms of designing such a device. As the experimental set-up was very flexible in torsion, the flexibility of the fin can be ignored. Therefore, flutter does not need to be considered as we are effectively dealing with a single degree of freedom system. However, the possibility of divergence still needs to be taken into account.

This analysis enabled various options in the design of the torsion bar to be considered. One of the main considerations that needed to be investigated was how great a difference between highest and lowest stiffness could be achieved. A target factor of 2 was felt by the investigators to be sufficient for demonstration of the principle. Similarly, it was felt that a goal of an efficiency of 2 would be a suitable target, which would enable the surface area of a new design to be halved – a substantial reduction.

Modelling of the Test Set-Up

Consider the idealised model of the wind tunnel model and attachment shown in figure 8.

A number of assumptions have been made in this analysis, due to the nature of the model, and also the low speed of the wind tunnel tests, it is not considered that too great an approximation has been made:

- The fin is considered to be rigid
- Dynamic aeroelastic aspects are ignored
- Strip theory aerodynamics is assumed with the lift acting on the quarter chord

- Simple torsion theory is applied to the torsion bars (made up of attachment to the fin and the variable length bar)
- The structure that the variable length torsion bar is attached to is considered to be rigid.

Although a number of assumptions have been made, the model allows various parameter studies to be made in order to develop the initial design.

Assuming that the fin is rigid, then all strips acting chordwise on the fin are at the same angle of incidence = initial incidence α + twist θ. The total moment acting on the fin is found by integrating the product of the aerodynamic force acting at the aerodynamic centre of each strip and its distance from the attachment point across the whole fin.

Mathematically this can be expressed in terms of the lengths of the sides of the fin A,B,C and the position of the attachment P, as

$$\text{Total Moment} = \frac{1}{2}\rho V^2 a_1 (\alpha + \theta) \int_0^A \left(B + \frac{(C-B)x}{A} \right) \left(-P + \frac{3}{4}\left(B + \frac{(C-B)x}{A} \right) \right) dx$$

where a_1 is the 2D lift curve-slope, ρ is air density and V the air-speed. Thus

$$\text{Total Moment} = \frac{1}{2}\rho V^2 a_1 (\alpha + \theta) \int_0^A -\left(B + \frac{(C-B)x}{A} \right) P + \left(\frac{3}{4}\left(B + \frac{(C-B)x}{A} \right)^2 \right) dx$$

Thus the total moment applied to the fin is found as

$$\frac{1}{2}\rho V^2 a_1 (\alpha + \theta) \left[\frac{A}{4(C-B)}(C^3 - B^3) - \frac{PA}{2}(C+B) \right] = \Phi(\alpha + \theta)$$

For equilibrium at a particular airspeed

$$K_\theta \theta = \Phi(\alpha + \theta)$$

so the angle of twist

$$\theta = \frac{\Phi \alpha}{K_\theta - \Phi}$$

and the divergence speed occurs when $K_\theta = \Phi$. Note that when the attachment is forward enough for the aerodynamic moment to become negative (i.e. Φ is negative), then the angle of twist θ becomes negative and divergence cannot occur.

It only remains to determine the torsional stiffness due to the bar, which is made up of two elements of the same material (in this case steel). The part attached between the fin and the torsion bar device (initially set as at length 26mm and with circular cross-section of diameter 20mm). The second part of the bar was set at a maximum total length of 20cm but this can be reduced using the torsion bar device; it can be of different square cross-section sizes.

The total twist for both bars, of shear modulus J, together subjected to torque T is

$$\theta = \frac{T}{G}\left(\frac{L_1}{J_1} + \frac{L_2}{J_2}\right)$$

and hence the torsional stiffness

$$K_\theta = \frac{G}{\left(\dfrac{L_1}{J_1} + \dfrac{L_2}{J_2}\right)}$$

Design of a Suitable Bar Cross-Section

As an initial illustration of how the torsion bar can be used to influence the static aeroelastic behaviour of the vertical tail, consider the case where the length of the 10mm sided bar is increased from 1cm to 20cm. Figure 9 shows the torsional stiffness, amount of twist for a 30 m/s airspeed and initial incidence of 1°, and divergence speed for the most rearward attachment position.

As predicted from previous studies, the lowest divergence speed is found at the rearmost attachment position, consequently this position must be considered for the design case.

Figure 10 shows the effect of taking the largest torsion bar length with the most rearwards attachment position for the 30 m/s case, and then changing the size of the torsion bar cross section (varying from 8.2mm to 12mm sides). It can be seen that by reducing the side dimension, the target of an efficiency of 2 can be met (t = 8.92mm), however, care must be taken not to reduce the dimension by too much as the divergence speed becomes less than 30 m/s (t = 8.07mm). Should a less ambitious efficiency target of 1.5 be set, then this is achieved with a side length of 9.16mm. Alternatively, the length of the torsion bar could be reduced.

For this work programme, it was decided to proceed initially with a torsion bar of sides 10mm, and following initial experiments, the tests continued with a 8mm sided bar. Unfortunately, because only non-hardened steel was available, there were permanent deformations for even moderate loads on the torsion bar. Another problem with this design was freeplay, which progressively grew after testing of the device. The attachment that slided was made out of brass for minimum friction, but each time the device operated, the torsion beam wore material out of the brass attachment, thus extending the freeplay (fig 11). Due to these difficulties, all wind tunnel tests using the torsion bar had to be abandoned. Both problems could be solved with the use of a teflon coated high strength steel bar, or a steel attachment, see the proposed design later in the report.

Bending Rods Design

The decision was made to go ahead with the bending rods designs shown in figs 7 and 12. After having made some initial tests with non-hardened steel that also after a certain twist had permanent deformation, stainless steel was used which performed much better.

Two sets of four rods different diameters (4.76mm and 7mm) were manufactured and hence have different stiffnesses for a given free length. As will be described in the results chapter, such a design behaves non-linearly and would not be used on a full-size aircraft.

Selection of Model Stiffnesses and Scale Factors

The stiffness was chosen such that (see figure 3) an efficiency of 2.0 at the 2300mm rearward attachment point of the full size fin could be reached at a speed of 0.09 M which corresponds to a speed of 30 m/s.   Now only the geometric scale factors of the wind tunnel model had to be considered being a 1:5 replica of the aircraft fin.

Dimension	Scaling factor	Units
Length	0.2	Mm
Stiffness	0.2	N/mm
Torsional Stiffness	0.2^{-3}	Nmm/rad
Frequency	5.0	Hz
Mass	0.2^{3}	Kilos
Velocity	1.0	m/s

Table 1. Scale factors

As can be seen from figure 3 at $5.1*10^{6}$ Nmm/rad, an efficiency of 2 is achieved corresponding to a model stiffness of $5.1*10^{6}*(0.2)^{3} = 40800$ Nmm/rad

Tests in the wind tunnel were performed varying the attachment stiffness around this value.

Results

Impulse Tests with Small Rods

Impulse tests were performed for the small rod solutions and wind tunnel tests were made to measure efficiencies and load alleviation factors for small and large rods for three attachment positions and three wind tunnel speeds.

Impulse tests were made for several wind tunnel speeds (0, 10, 20 and 30 m/s) and different rod lengths. The natural frequencies were measured at each test point, and it was found that there was significant non-linear change in the stiffness values corresponding to a linear change in length. The three lengths considered gave stiffnesses of high (124324 Nmm/rad), medium (54769 Nmm/rad) and low (46000Nmm/rad).

In figures 13 – 24, impulse responses of three stiffness arrangements are shown for various speeds. Results of these tests are plotted in figures 25 – 27. As was already indicated by the stiffness behaviour, non-linear behaviour is shown when speeds are reaching 30 m/s and an undamped vibration appears.

Efficiencies

Efficiency for an airfoil is defined as

$$\eta = \frac{C_{L_{\alpha_{elastic}}}}{C_{L_{\alpha_{rigid}}}}$$

In essence this means if a preset angle of the fin, say 5° increases to 10° at a certain speed, then we have an efficiency of 2. If it decreases to 2.5^o, then the efficiency is 0.5. In airplanes with forward sweep designs, efficiency goes above 1 with speed – therefore divergence could occur. With swept-back designs, efficiency normally goes below one and sometimes even control surface reversal can happen.

In our design, we are trying to increase efficiency for the cruise speed range by aeroelastic tailoring with carbon fibre composites, and for low speeds by reducing the attachment stiffness.

Efficiences for Low Stiffness Rods

In figure 28 all the results are presented in a table. Figs 29 to 31 show efficiencies for various attachment positions and different wind tunnel speeds. A maximum efficiency of 1.93 could be reached.

Efficiencies for High Stiffness Rods

Figures 32 to 34 show efficiencies for various attachment positions and different wind tunnel speeds. The highest efficiency achieved was 1.83.

Discussion of Results

With the manufactured variable stiffness devices it was possible to achieve efficiencies of around 2.0 at the stiffness level predicted analytically (see figure3). Applying the scale factor of table 1, one gets 40800Nmm/rad for efficiency of 2.0 for the model. Results from the torsion bar wind tunnel tests could not be used because they demonstrated freeplay and strength problems. The four bar solutions could reach efficiencies of 2.0 but were highly non-linear with free length (due to the stiffening mechanism). There were also strength problems with the smaller diameter rods.

Proposed Aircraft Solution

Looking at figure 2 it can be seen that for the most rearward attachment position, a stiffness of about $1*10^8$ Nmm/rad will lead to divergence around 100 m/s and hence to high efficiencies >1 whereas a stiffness of about $1*10^{10}$ Nmm/rad will clear the fin from flutter up to 450 m/s. This means that for landing at about 150 kts an efficient design against side wind is available reaching 900kts clearance speed for flutter with the high stiffness. Such a device is available with an inverted cone shown in figure 35, which is shown here in a set-up that is allows either the high or low stiffness to occur, but no intermediate values.

A finite element calculation was performed for this case (see figure 36). In figure 37 radial deflection is plotted versus length of the cone (3cm diameter at 0 going to 10cm at 20cm length). For the attachment area, a stiffness of $8.25*10^9$ Nmm/rad and for the full length stiffness of $2.91*10^8$ could be deduced. Looking at figure 2 again this will fulfill the requirements. Loads

for the low stiffness are low due to low landing speed airloads. The whole device could also be used for a fin and rudder with a gear ratio of about 1:3 since then the rudder would be in a linear aerodynamic regime.

Conclusions

A vertical tail wind tunnel model with variable torsional stiffness attachments was bench and also wind tunnel tested to examine the capabilities of the adaptive stiffness attachments. There were some setbacks on the actual designs which led to excessive freeplay and permanent deformations, however, successful testing was achieved in one of the test set-ups and it was shown that it is possible to control the torsional stiffness with the manufactured device. Comparisons with results from the analytical studies correlated well. An improved design of the adaptive attachment has been made which will fulfill the requirements for such a device.

<u>References</u>

1. Pendleton E, „Back to the future – How Active Aeroelastic Wings are a Return to Aviations Beginning and A Small Step to Future Bird Like Wings" NATA RTO Meet,. Braunschweig May 2000.
2. Pendleton E, Sanders B, Flick P & Sensburg O, Controllable Aeroelastic Lifting Surfaces. A Return to Aviations Beginnings and a Step Closer to Nature" IFASD 2001 pp555 – 566.
3. Tischler VA, Venkayya VB & Sensburg O, 'Aeroelastic Tailoring of Enpennage Structures' 41st SDM Conf April 2000.
4. Bureerat S, Cooper JE & Sensburg O, „Aeroelastic Optimisation of an Aircraft Fin Structure" 2nd ASMO Conference, Swansea, June 2000.
5. Cooper, JE, Bureerat S, Sensburg O & Dimitriadis G, „Aeroelastic and Structural Design of an All-Moveable Aircraft Fin" CASE Conference on Multidisciplinary Aircraft Design and Optimisation" June 2001.pp 177 – 184.
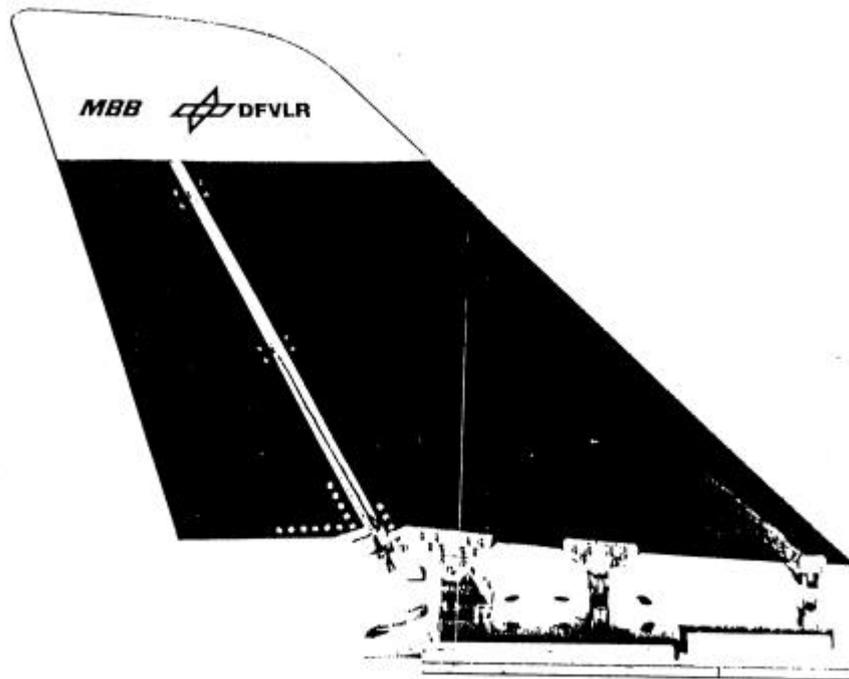
Figure 1. Aeroelastic Fin Model
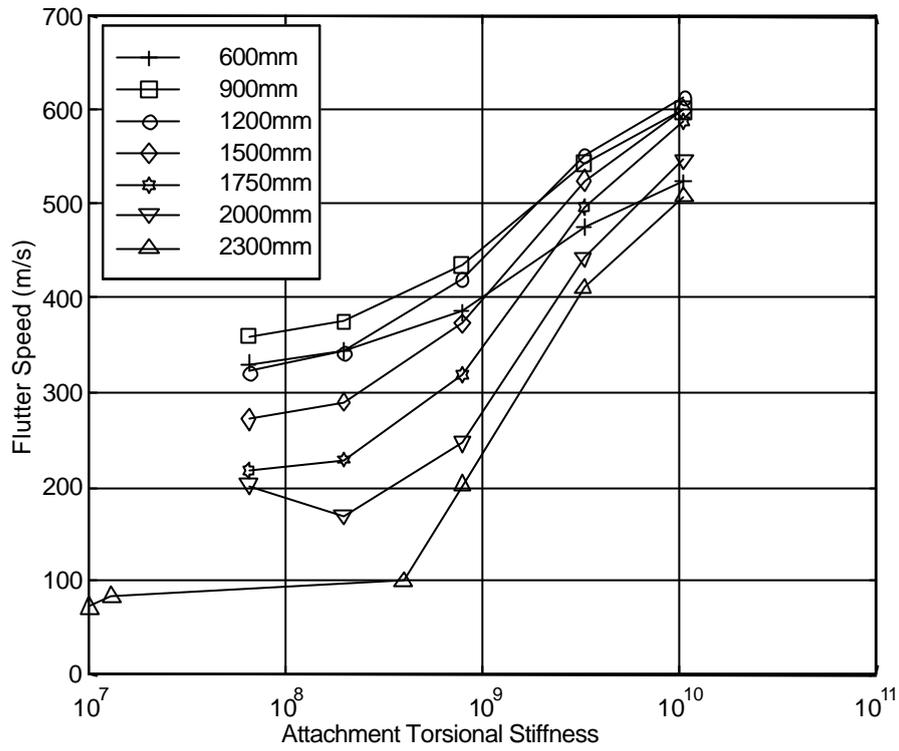
Figure 2. Variation of flutter / divergence speed for different attachments

Fin Efficiency Vs Torsional Stifness at 2300mm Attachment Point (Aircraft)
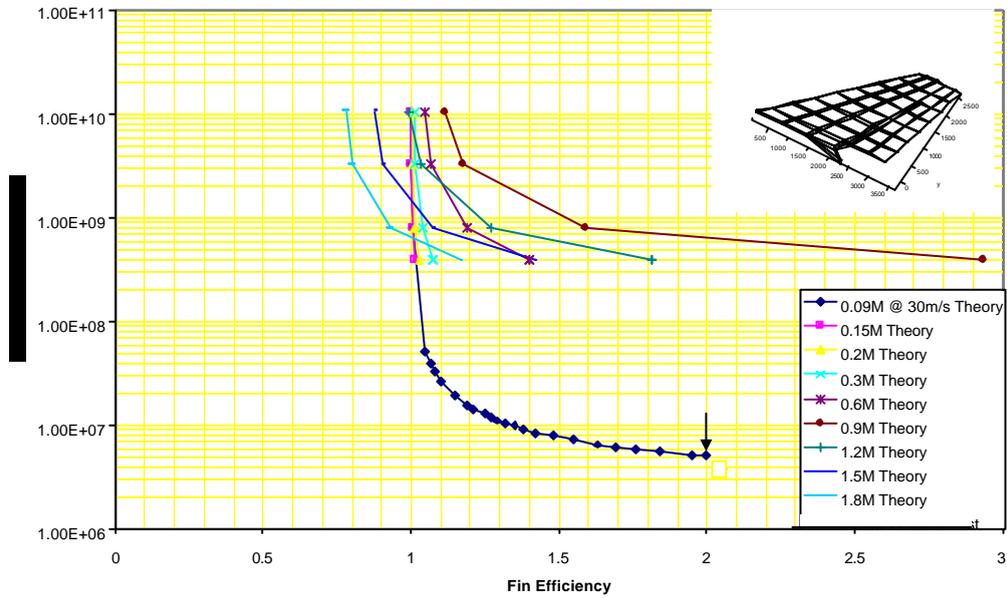
Figure 3. Selection of springs for wind tunnel test (arrow indicates stiffness of 5.1×10^6)
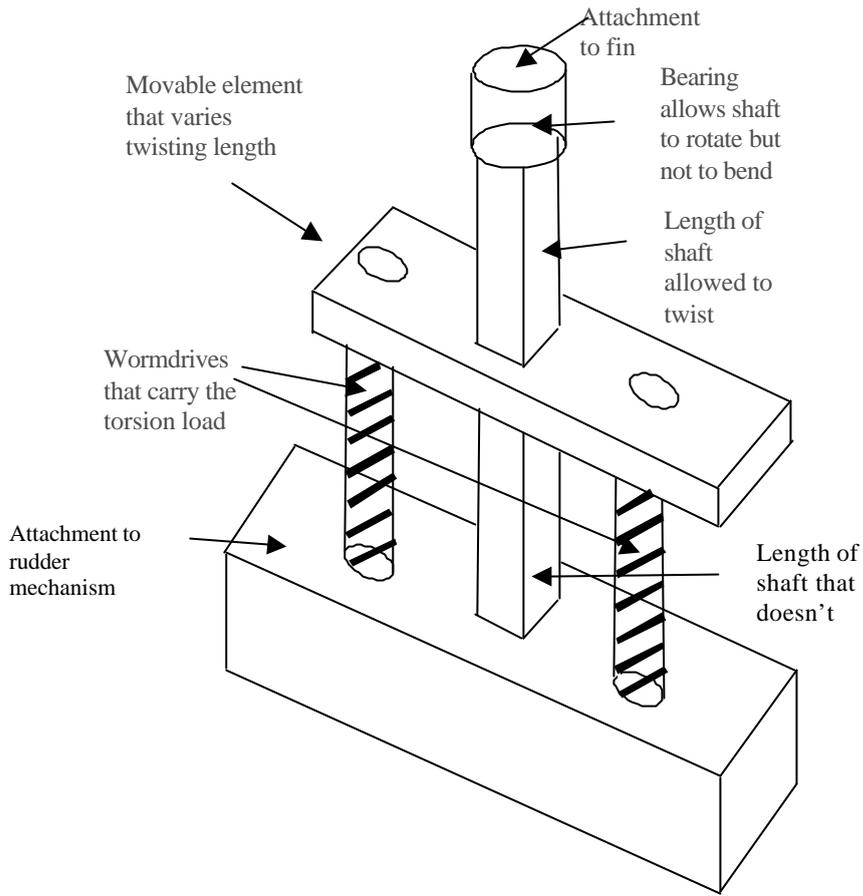
Figure 4. Proposed Variable Stiffness Torsion Beam Concept
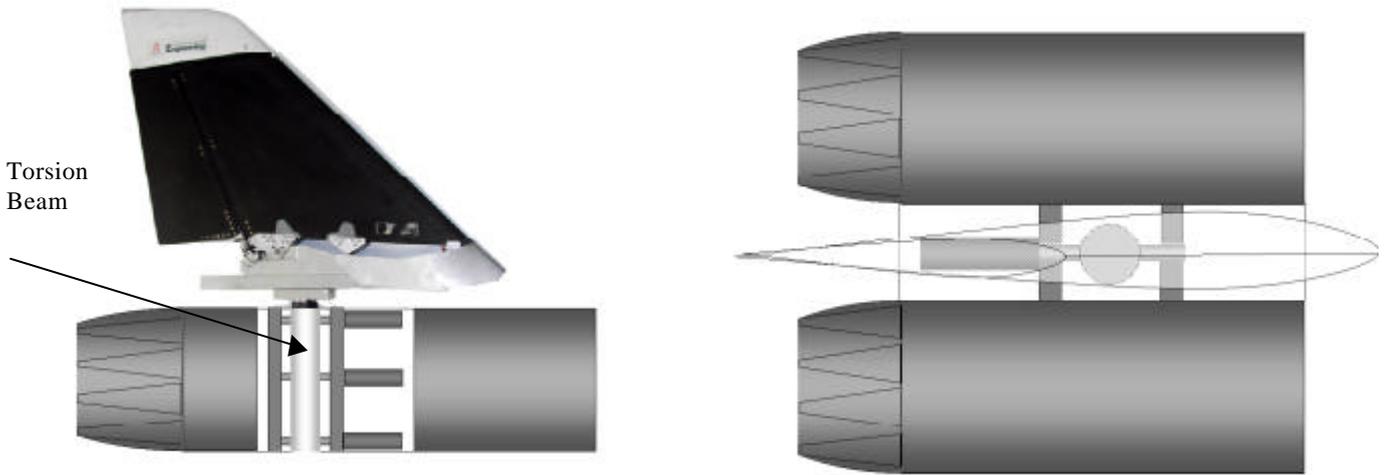
5a. Side view   5b. Plan view

Figure 5. Idealised Application of Concept on Full-Size Aircraft

Figure 6.   Manufactured Adaptive Stiffness Torsion Bar Concept.

Figure 7.   Manufactured Adaptive Stiffness Four Rods Concept.
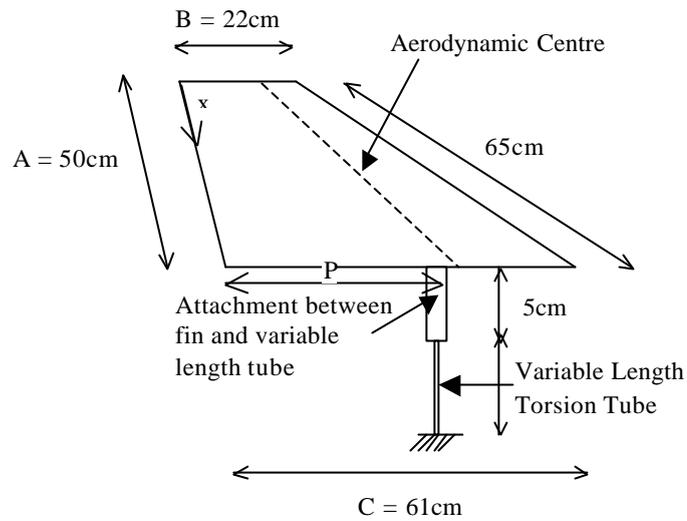
Figure 8. Schematic For Mathematical Model of the Vertical Tail
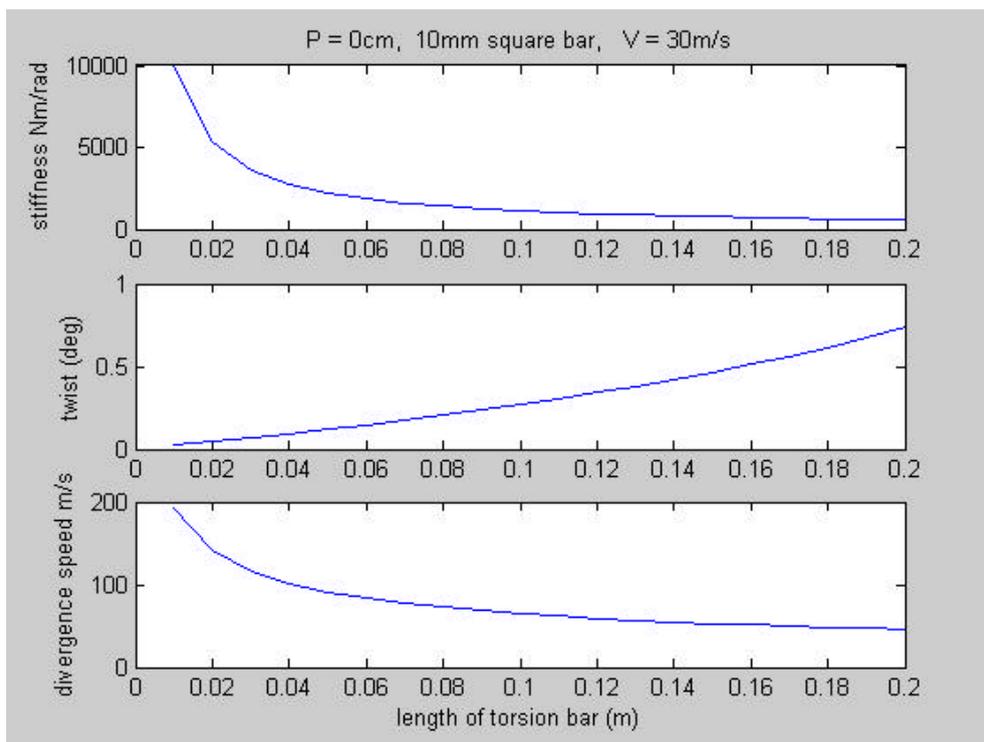
Figure 9.   Torsional Stiffness, Twist and Divergence Speed for 10mm Square Bar, 30m/s, P=0.
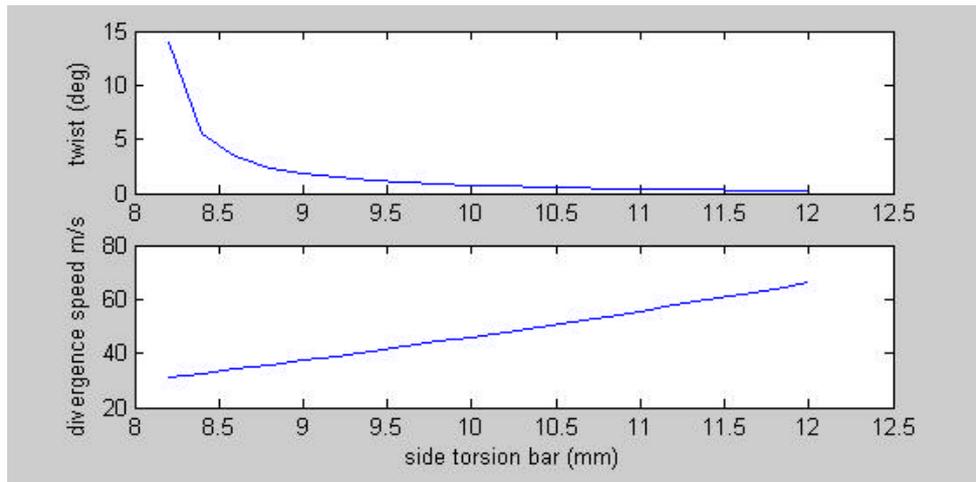
Figure 10. Effect of Varying Bar Dimensions on Twist and Divergence Speed.
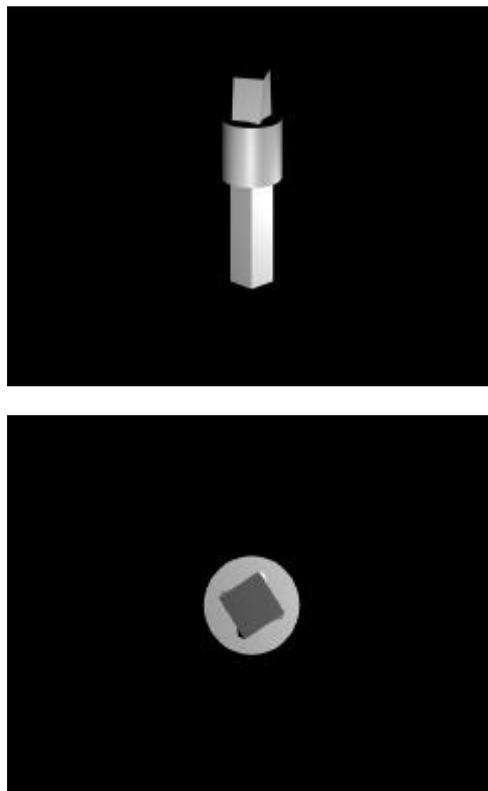
Figure 11. Illustration of FreePlay Due to Wear of Brass Sleeve.
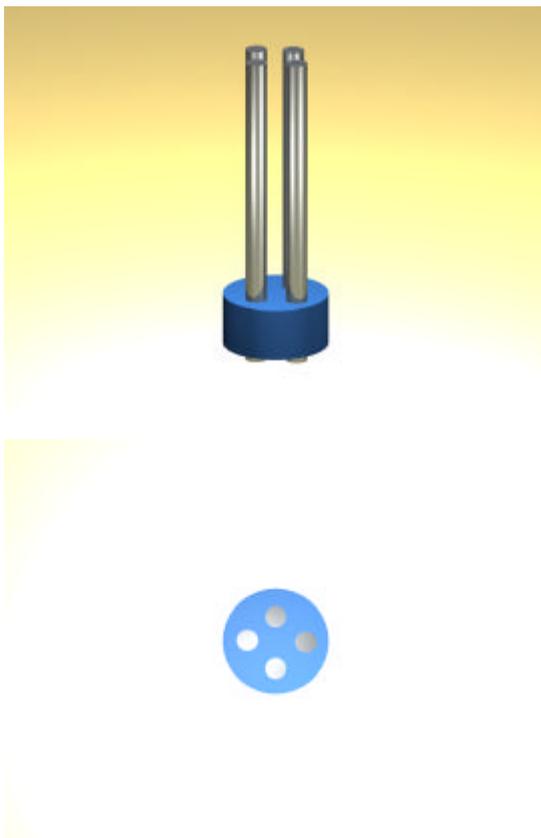
Figure 12. Sleeve Arrangement for the Four Rods Concept

IMPULSE RESPONSE WAVEFORM (LOW STIFFNESS)
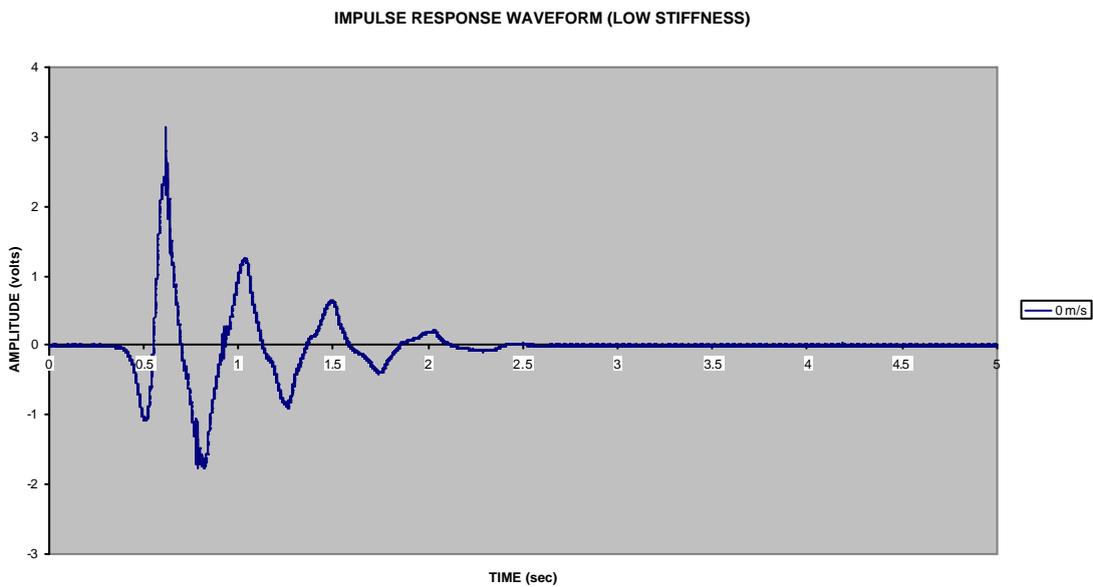
Figure 13. Impulse Response. Four rods (4.76mm). 46000Nmm/rad. Zero Speed.

IMPULSE RESPONSE WAVEFORM (MEDIUM STIFFNESS)
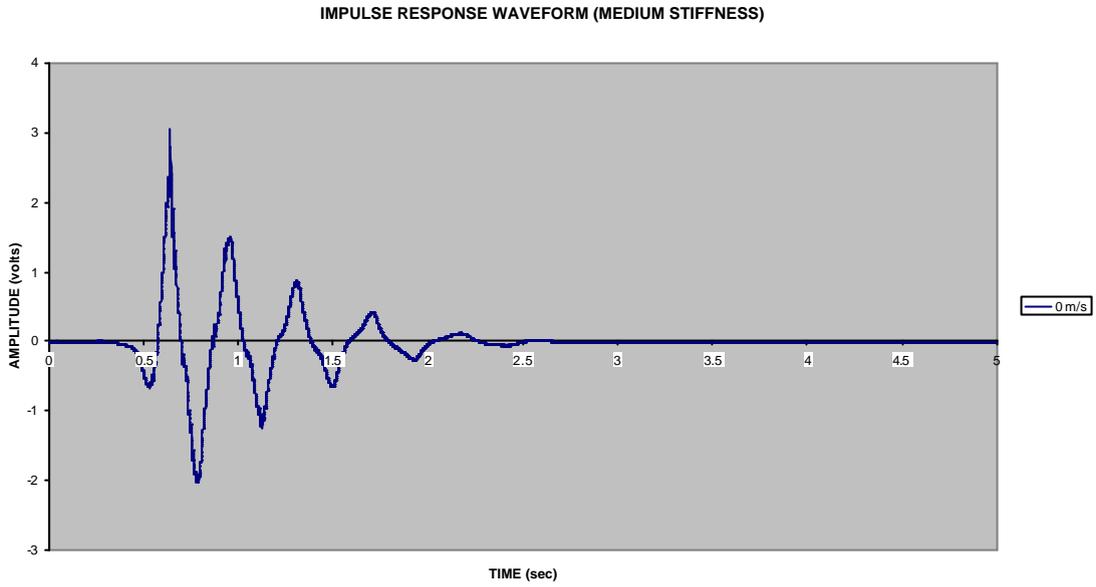
Figure 14. Impulse Response. Four rods (4.76mm). 54760 Nmm/rad. Zero Speed.

IMPULSE RESPONSE WAVEFORM (HIGH STIFFNESS)
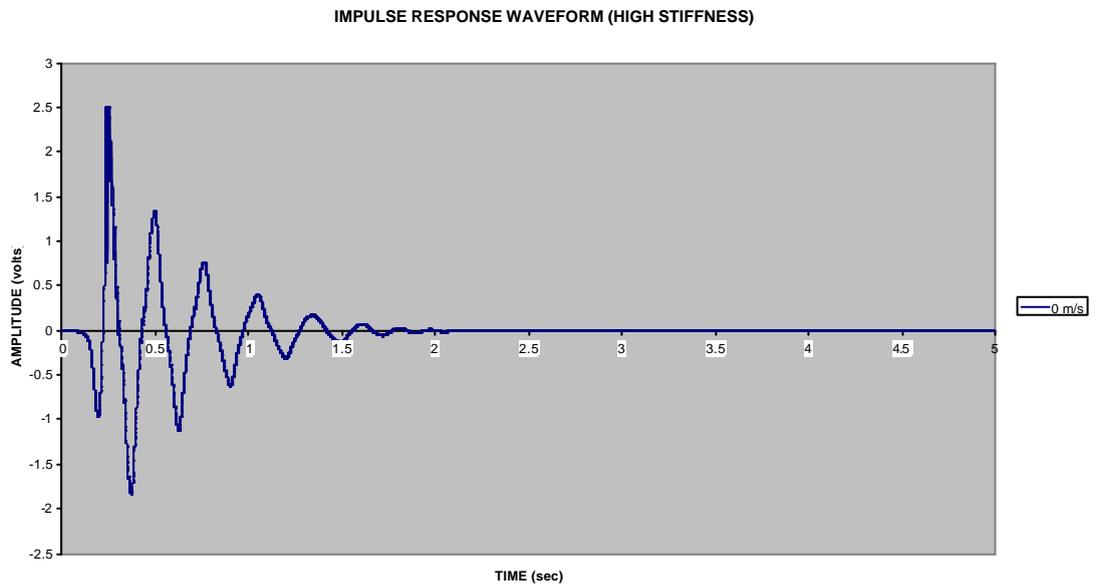
Figure 15. Impulse Response. Four rods (4.76mm). 124324 Nmm/rad. Zero Speed.

IMPULSE RESPONSE WAVEFORM (LOW STIFFNESS)
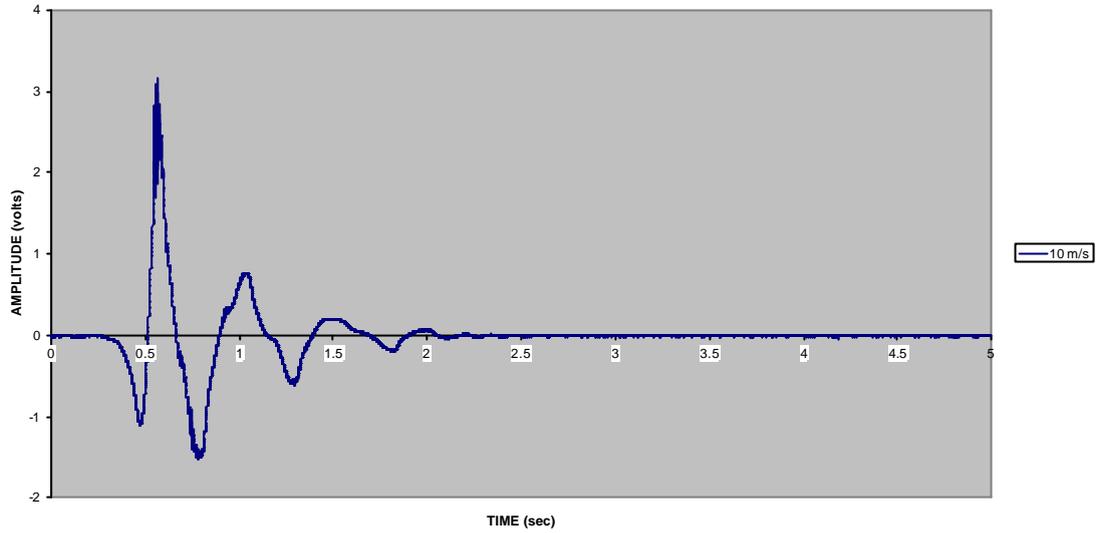
Figure 16. Impulse Response. Four rods (4.76mm). 46000 Nmm/rad. 10m/s.

IMPULSE RESPONSE WAVEFORM (MEDIUM STIFFNESS)
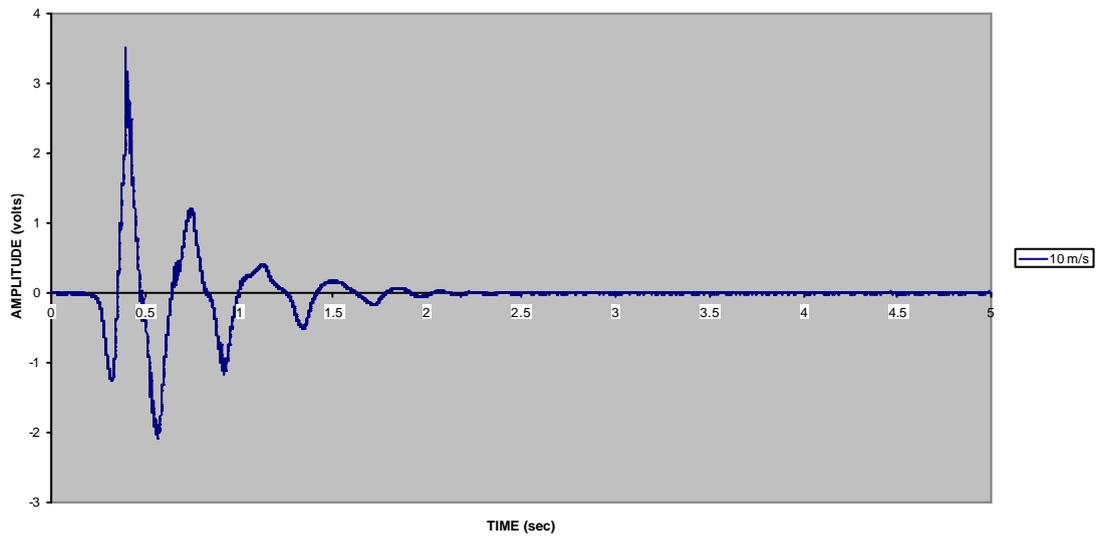
Figure 17. Impulse Response. Four rods (4.76mm). 54760 Nmm/rad. 10m/s.

IMPULSE RESPONSE WAVEFORM (HIGH STIFFNESS)
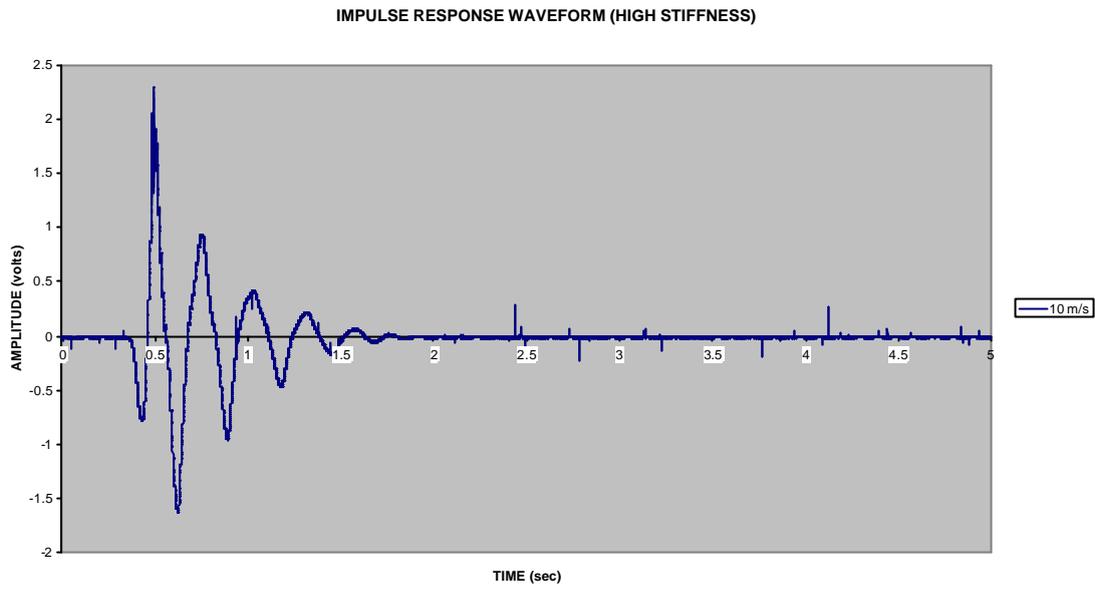
Figure 18. Impulse Response. Four rods (4.76mm). 124324 Nmm/rad. 10m/s.

IMPULSE RESPONSE WAVEFORM (LOW STIFFNESS)
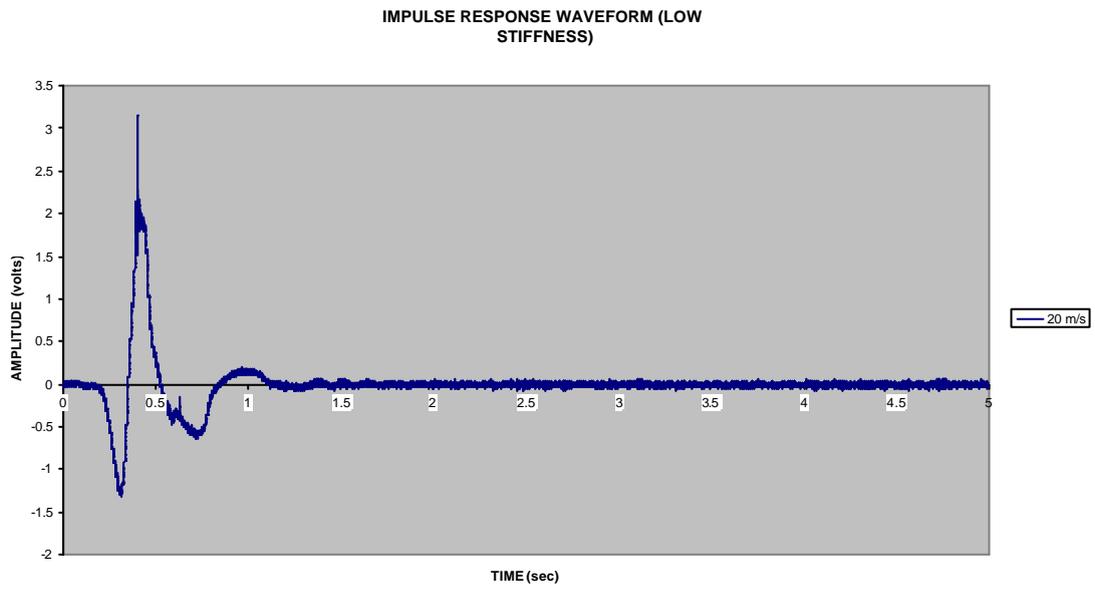
Figure 19. Impulse Response. Four rods (4.76mm). 46000 Nmm/rad. 20m/s.

IMPULSE RESPONSE WAVEFORM (MEDIUM STIFFNESS)
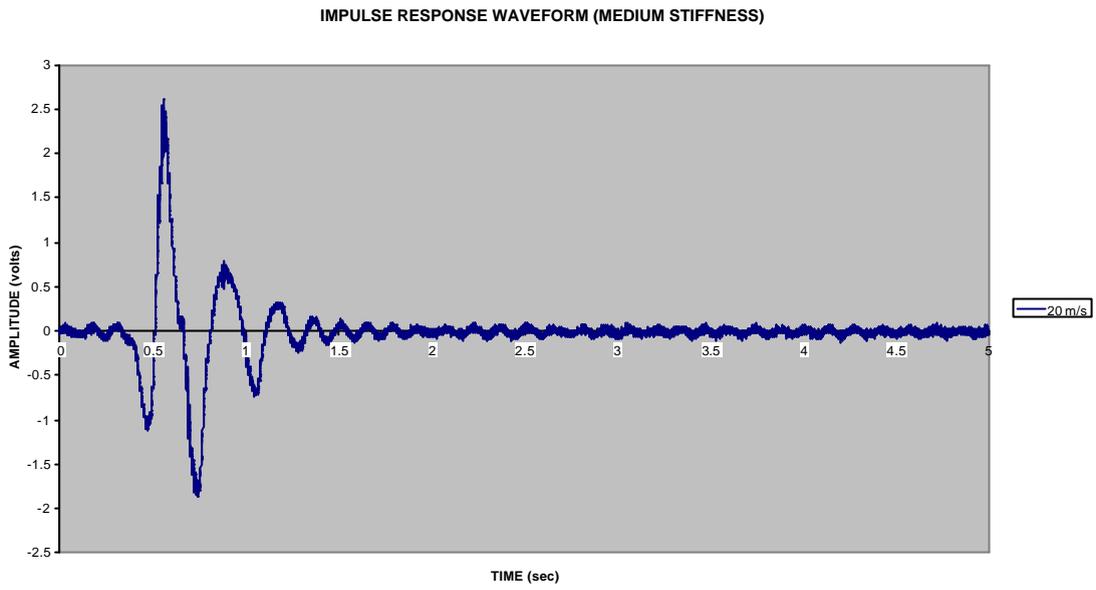
Figure 20. Impulse Response. Four rods (4.76mm). 54760 Nmm/rad. 20m/s.

IMPULSE RESPONSE WAVEFORM (MEDIUM STIFFNESS)
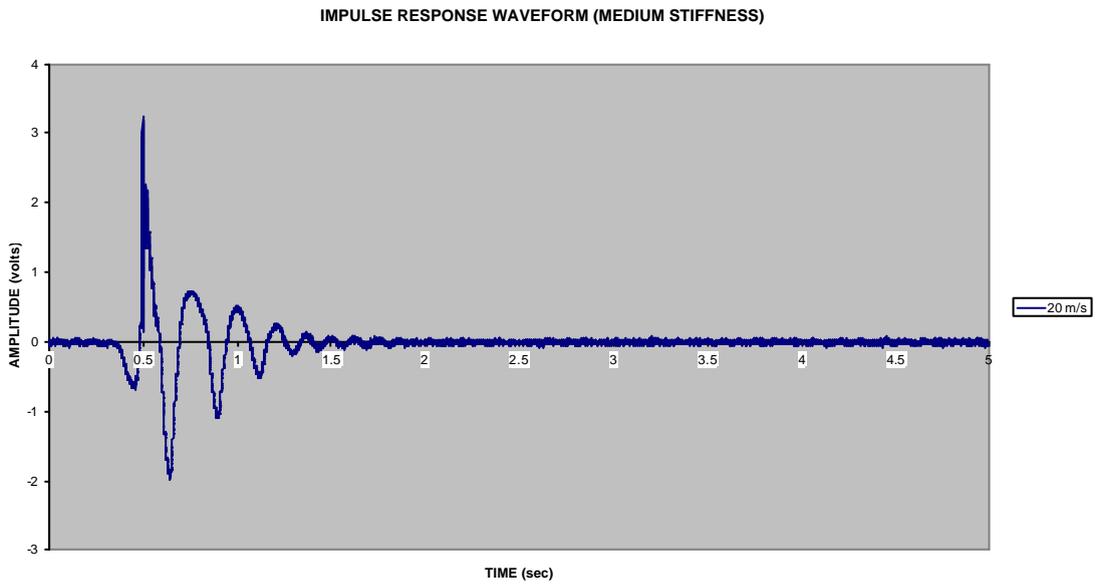
Figure 21. Impulse Response. Four rods (4.76mm). 124324 Nmm/rad. 20m/s.

IMPULSE RESPONSE WAVEFORM (LOW STIFFNESS)
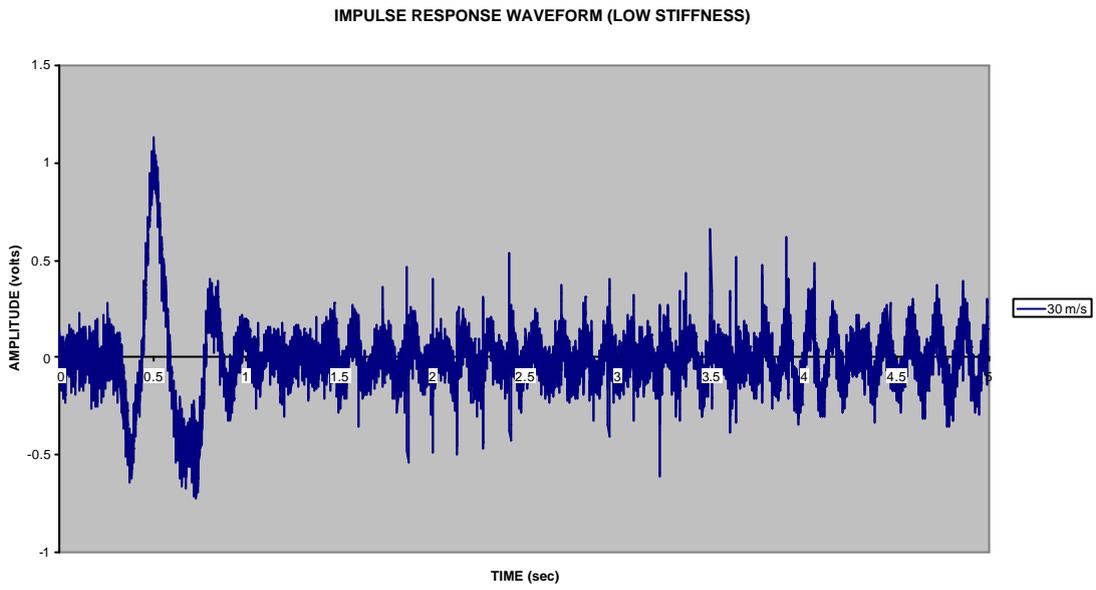
Figure 22. Impulse Response. Four rods (4.76mm). 46000 Nmm/rad. 30m/s.

IMPULSE RESPONSE WAVEFORM (MEDIUM STIFFNESS)
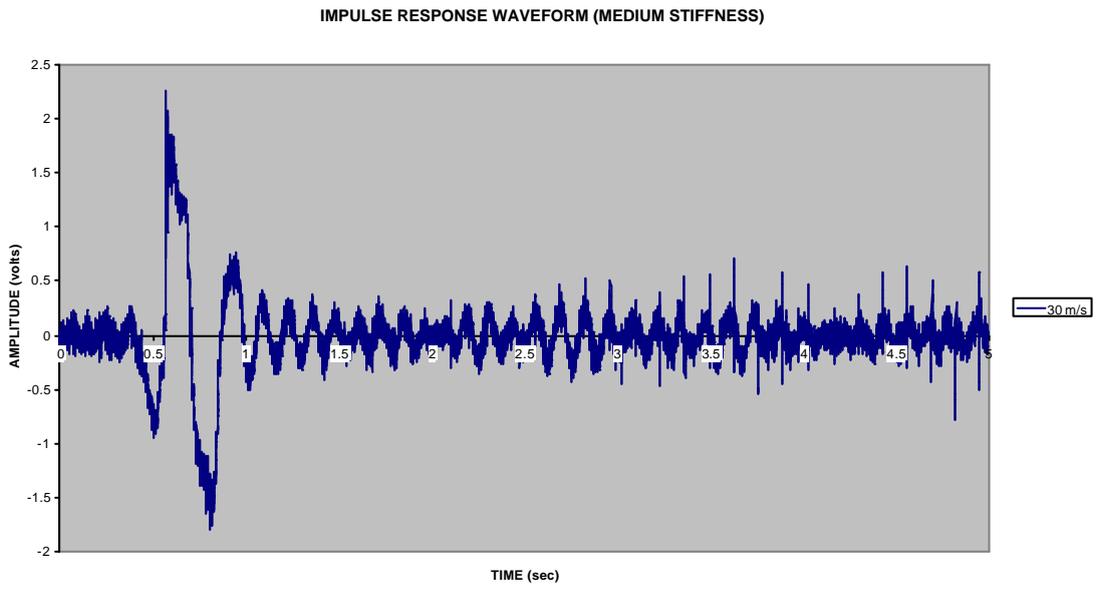
Figure 23. Impulse Response. Four rods (4.76mm). 54760 Nmm/rad. 30m/s.

IMPULSE RESPONSE WAVEFORM (HIGH STIFFNESS)
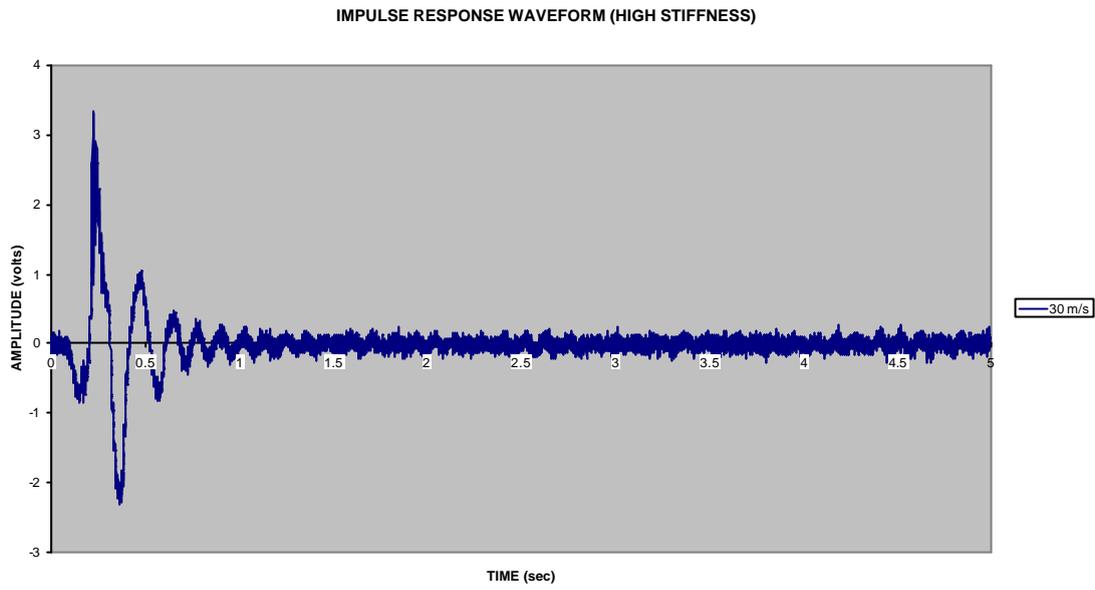
Figure 24. Impulse Response. Four rods (4.76mm). 124324 Nmm/rad. 30m/s.
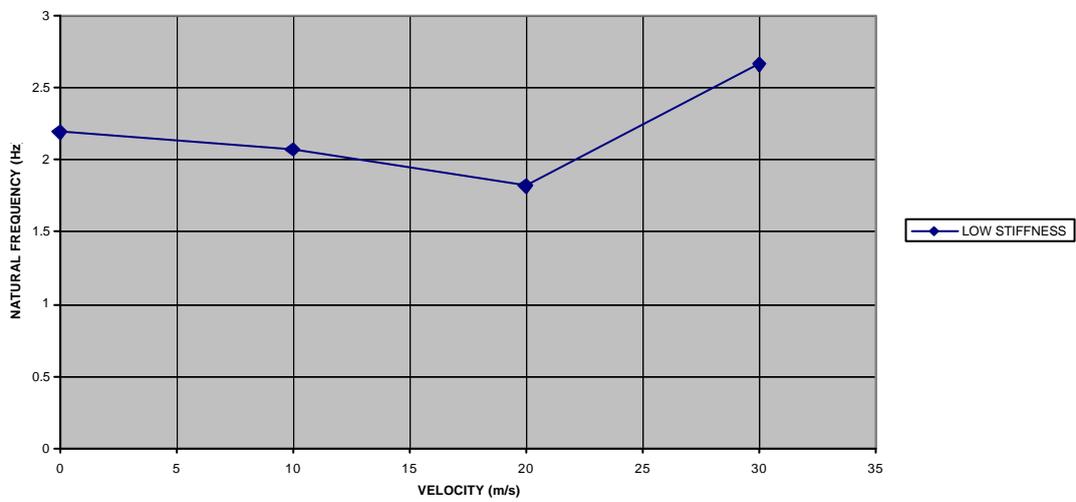
Figure 25. Natural Frequencies vs. Velocity.   46000 Nmm/rad
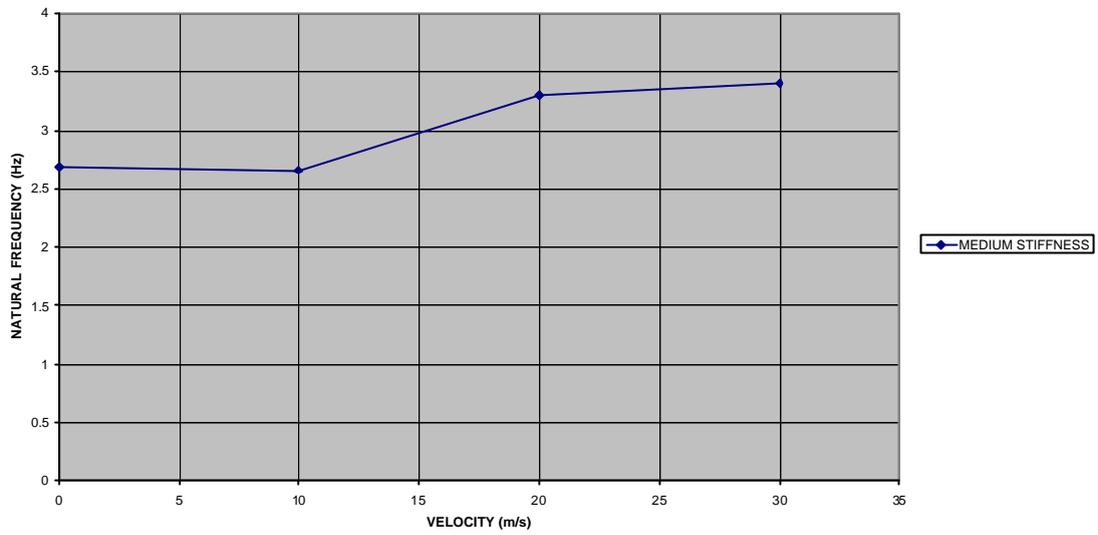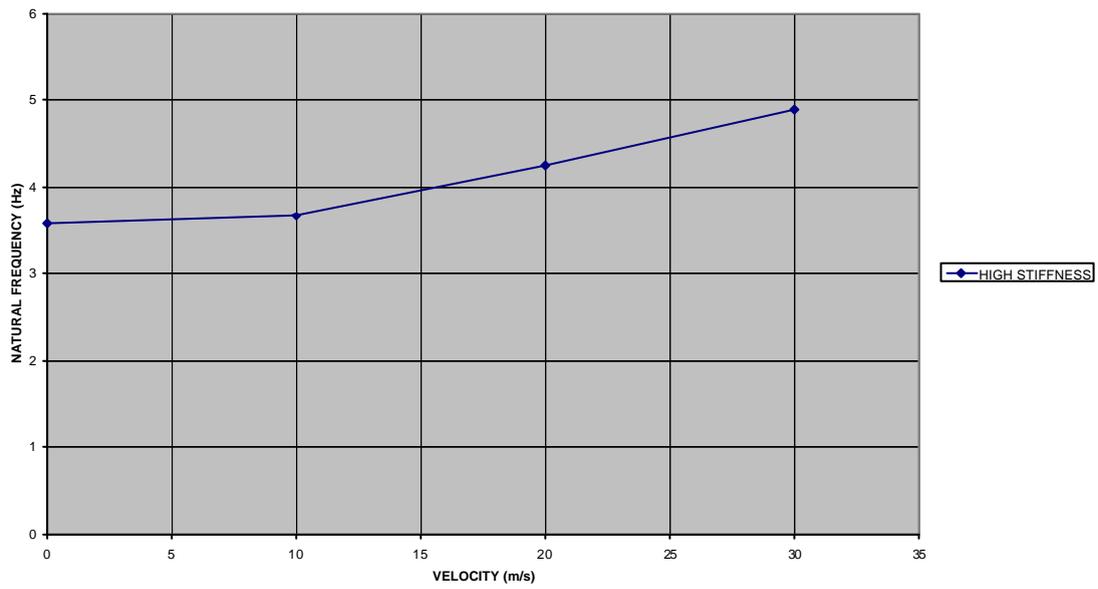
Figure 26. Natural Frequencies vs. Velocity.   54760 Nmm/rad

Figure 27. Natural Frequencies vs. Velocity.   124324 Nmm/rad

460mm rear attachment								
46000Nmm/rad	Preset Angle 15°		54760Nmm/rad	Preset Angle 14°		124324Nmm/rad	Preset Angle 11°	
Elastic Angle	Speed	Efficiency	Elastic Angle	Speed	Efficiency	Elastic Angle	Speed	Efficiency
0	0	1	0	0	1	0	0	1
1.5	10	1.1	0.5	10	1.03	0.5	10	1.04
6	20	1.4	3.5	20	1.25	2	20	1.18
14	30	1.93	7.5	30	1.53	4	30	1.36
300mm middle attachment								
46000Nmm/rad	Preset Angle 10°		54760Nmm/rad	Preset Angle 11°		124324Nmm/rad	Preset Angle 11°	
Elastic Angle	Speed	Efficiency	Elastic Angle	Speed	Efficiency	Elastic Angle	Speed	Efficiency
0	0	1	0	0	1	0	0	1
-0.5	10	0.95	-.5	10	.95	-.3	10	.97
-2.5	20	.75	-2	20	.81	-1	20	.9
-4	30	.6	-3.5	30	.77	-2	30	.81
120mm forward attachment								
46000Nmm/rad	Preset Angle 9.5°		54760Nmm/rad	Preset Angle 9.5°		124324Nmm/rad	Preset Angle 10°	
Elastic Angle	Speed	Efficiency	Elastic Angle	Speed	Efficiency	Elastic Angle	Speed	Efficiency
0	0	1	0	0	1	0	0	1
-3	10	0.72	-2.5	10	.77	-1.5	10	.85
-5	20	.47	-4.5	20	.52	-3	20	.7
-6	30	.31	-5.5	30	.42	-4	30	.6

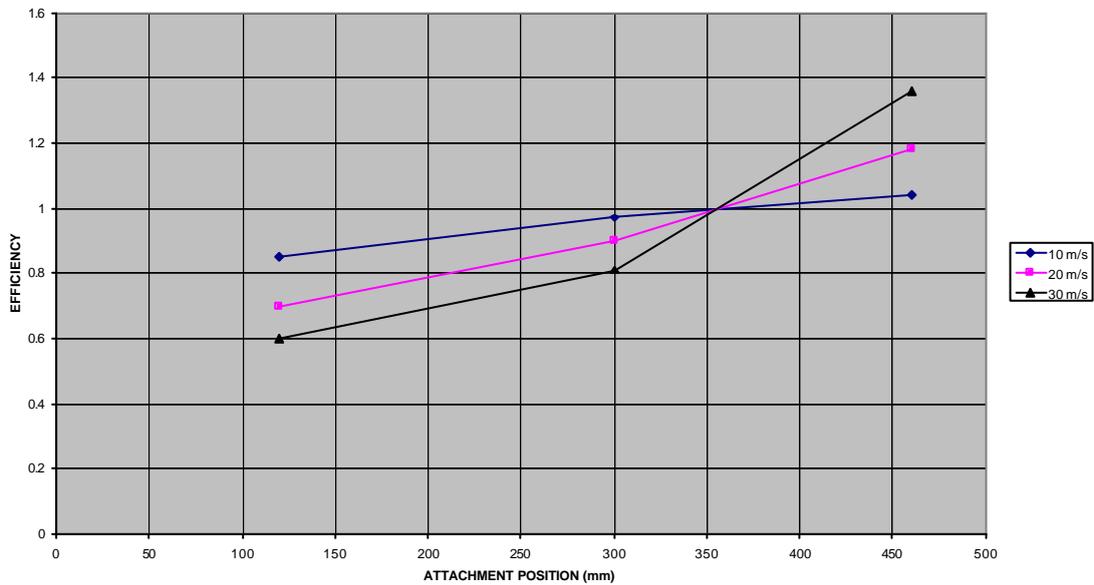Figure 28. Table of Efficiencies for 4.76mm Diameter Rods

Figure 29. Fin Efficiency vs. Attachment Position. 4.76mm Diameter Rods. 124324Nmm/rad.
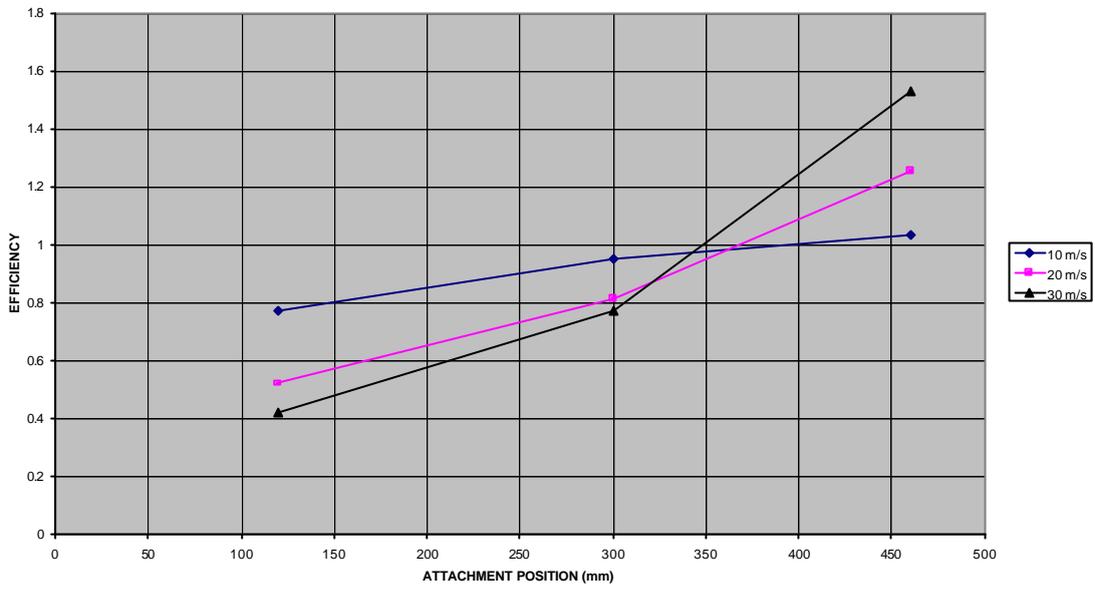
Figure 30. Fin Efficiency vs. Attachment Position. 4.76mm Diameter Rods. 54760Nmm/rad.
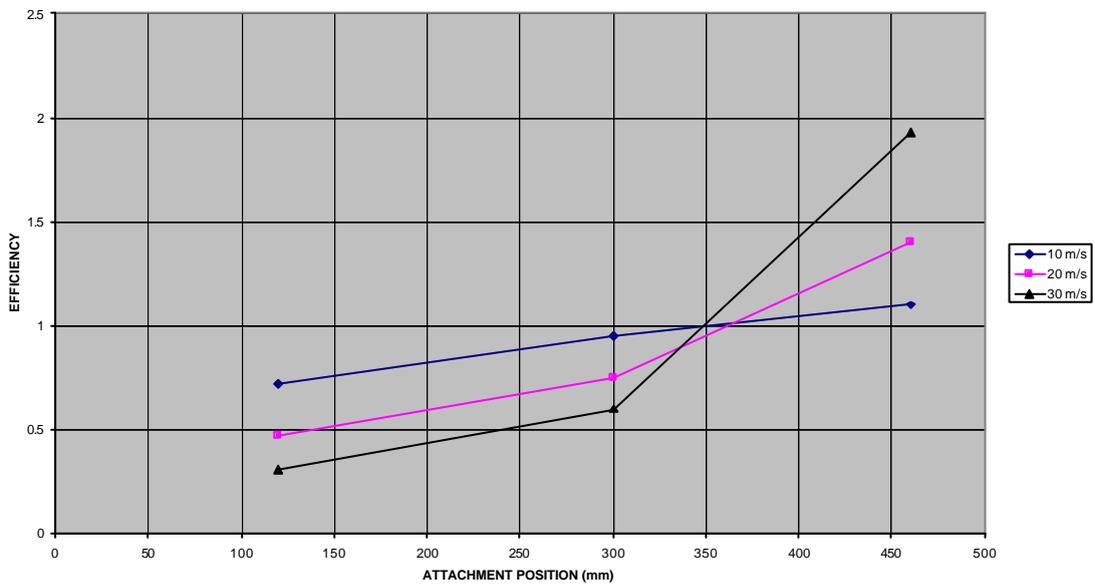

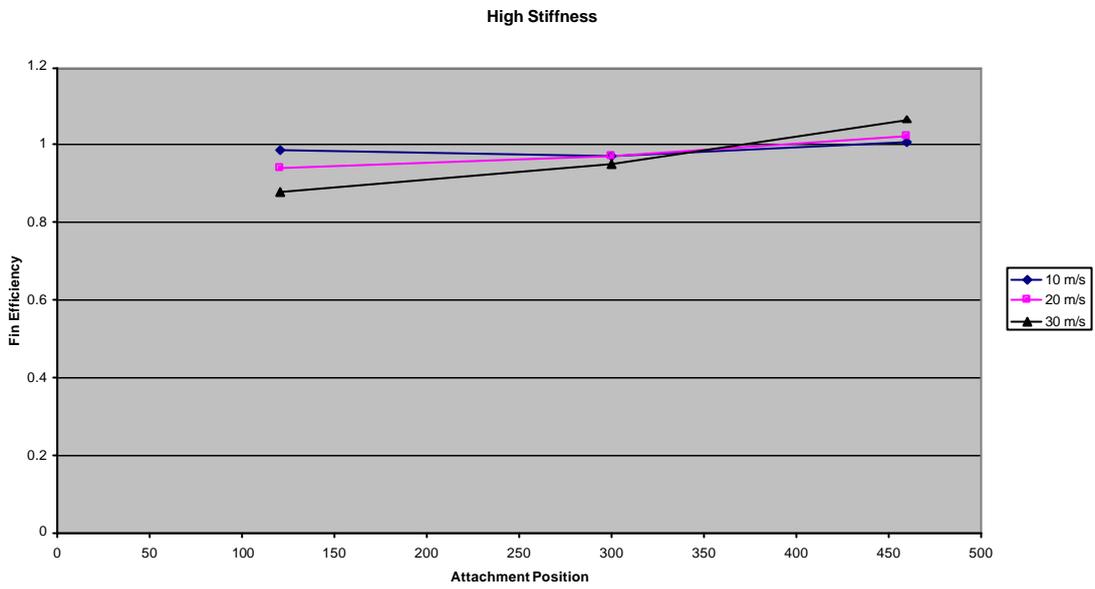Figure 31. Fin Efficiency vs. Attachment Position. 4.76mm Diameter Rods. 46000Nmm/rad.

High Stiffness

Figure 32. Fin Efficiency vs. Attachment Position. 7mm Diameter Rods. 88200Nmm/rad.
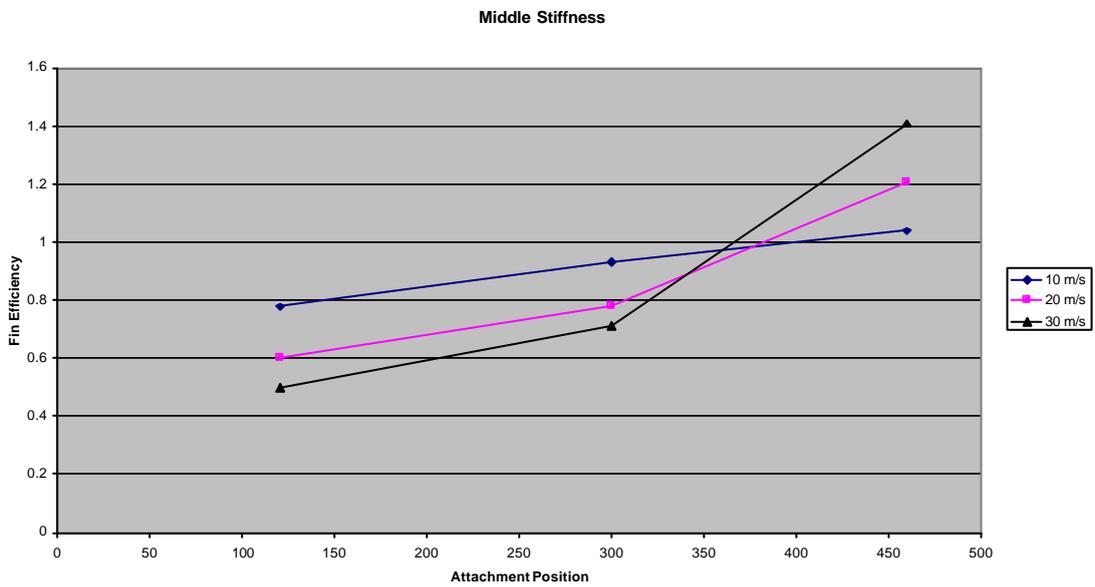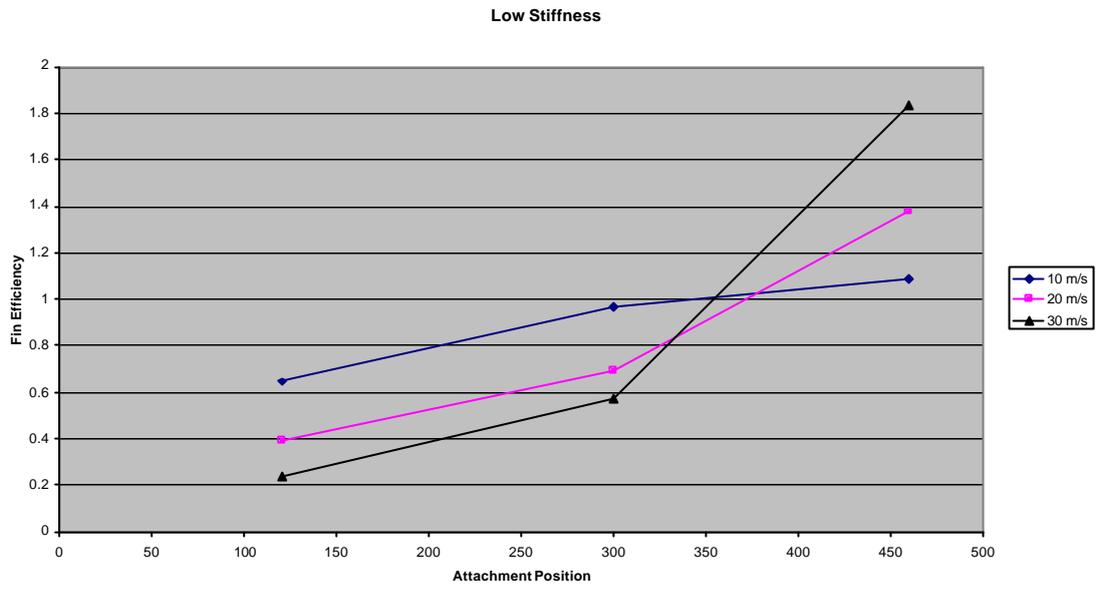
Middle Stiffness

Figure 33. Fin Efficiency vs. Attachment Position. 7mm Diameter Rods. 66150Nmm/rad.
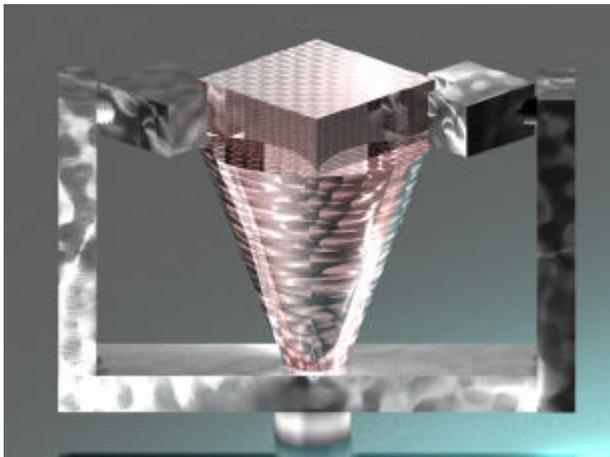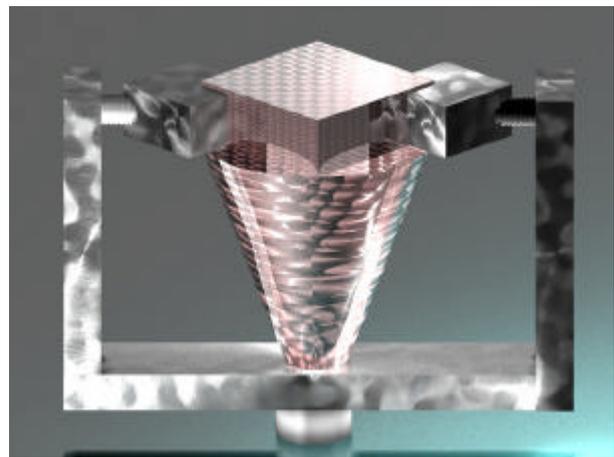
Figure 34. Fin Efficiency vs. Attachment Position. 7mm Diameter Rods. 44100Nmm/rad.

Lowest stiffness   highest stiffness

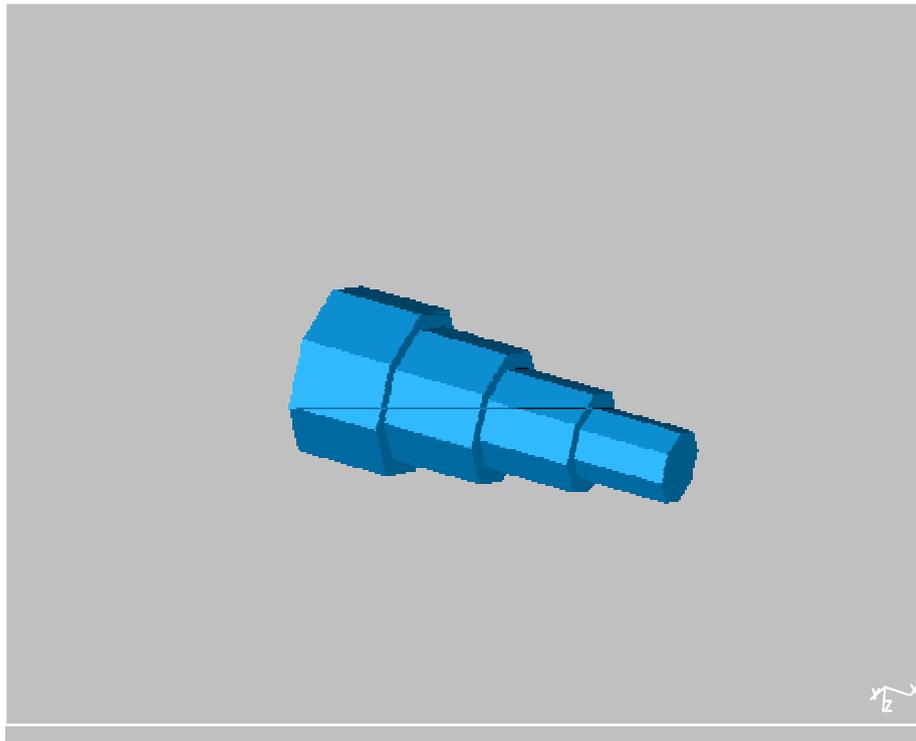Figure 35. Inverted Cone Adaptive Stiffness Attachment
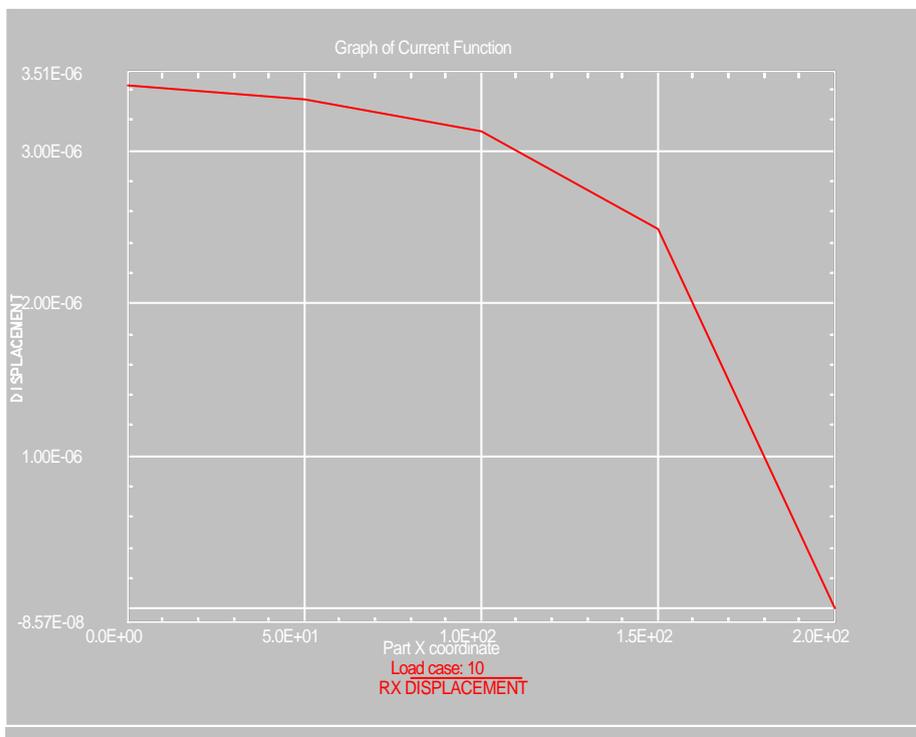
Figure 36 Finite Element Idealisation

Figure 37 Radial Deflection for Torsional Moment of 1000Nmm

ADDENDUM TO THE FINAL REPORT

A VARIABLE STIFFNESS CONCEPT FOR EFFICIENT VERTICAL TAIL DESIGN

EOARD CONTRACT FA 8655-02-1-3085

TASK 4 CONSIDERATIONS ON THE EXTENSION OF THE DESIGN FOR FULL SIZE AIRCRAFT AND QUANTIFICATION OF THE BENEFITS

<u>Extension of wind tunnel model test results to full size aircraft</u>

An inverted cone for the attachment of the fin was designed which is shown in Figure 1. The cone dimensions are 3 cm at the root going to 10 cm at 20 cm length. Such a device would easily fit into any two engined fighter fuselage, which has about a diameter of 1 metre (Figure 2).

In the report it is deduced that for the most rearward attachment position, a stiffness of about $1*10^8$ Nmm/rad will lead to divergence around 100 m/s and hence to high efficiencies >1 whereas a stiffness of about $1*10^{10}$ Nmm/rad will clear the fin from flutter up to 450 m/s. This means that for landing at about 150 kts an efficient design against side wind is available reaching 900kts clearance speed for flutter with the high stiffness.

A finite element calculation was performed for this case. For the attachment area, a stiffness of $8.25*10^9$ Nmm/rad and for the full length stiffness of $2.91*10^8$ could be deduced. This numbers will fulfil the requirements as stated above.

Accessing the weight of the modifications for an all movable fin plus adaptive stiffness is very difficult to achieve without having a real project application.

It was shown in EOARD REPORT F61775-01-WE081, "Design, Fabrication, Ground Resonance and Wind Tunnel Test of a Model for an Efficient All-Moveable Fin Design for Aircraft", an increase in efficiency for a fin to twice its rigid value is

possible. Therefore the weight of the fin could be halved but we have to pay some extras for making an all-movable fin and also for the variable stiffness.

Based upon the above simple analysis, it can be assumed that 20% of a typical fin weight could be saved by applying this new concept.
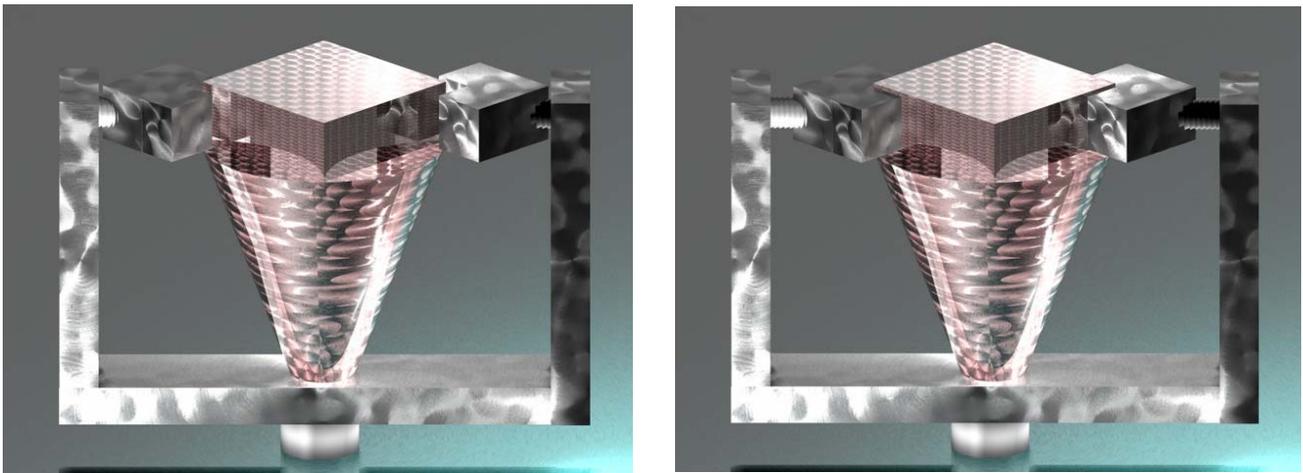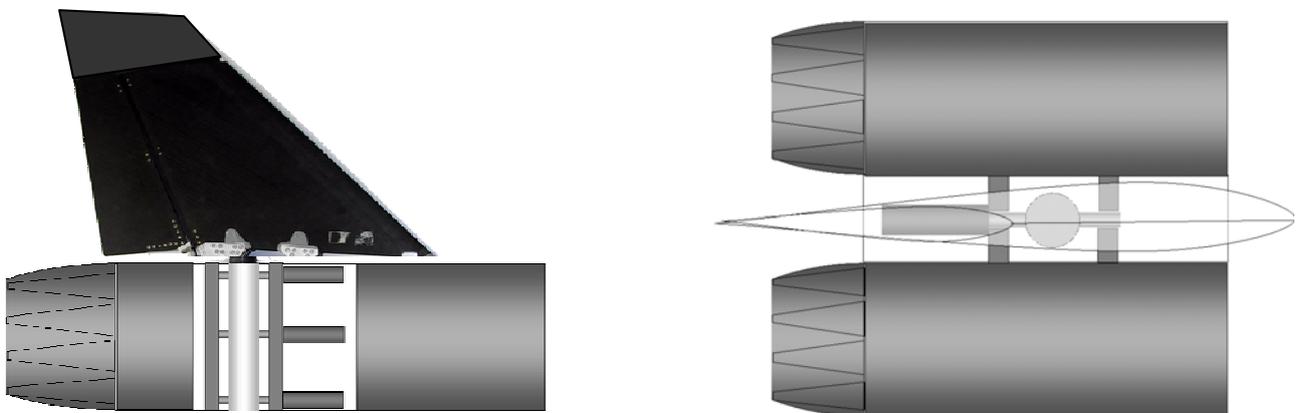

Figure 1. Inverted Cone Adaptive Stiffness Attachment

Figure 2. Idealised Application of Concept on Full-Size Aircraft